Türk Doğa ve Fen Dergisi
Turkish Journal of Nature and Science

Use of New Natural Dyes Extracted from Different Sections of *Salvia urica* in Dye-Sensitized Solar Cells

Fehmi ASLAN[1]* , Halil İbrahim YAMAÇ[2]

[1] MTU University, Yeşilyurt MYO, Department of Motor Vehicles and Transportation Technologies, Malatya, Türkiye
[2] Firat University, Technologies Faculty, Department of Mechatronics Engineering, Elazığ, Türkiye
Fehmi ASLAN ORCID No: 0000-0002-5304-0503
Halil İbrahim YAMAÇ ORCID No: 0000-0002-4628-0971

*Corresponding author: fehmi.aslan@ozal.edu.tr

Abstract: In this study, natural dyes that were obtained from the branches, flowers and leaves of *Salvia urica* were utilized as sensitizers in TiO_2-based dye-sensitized solar cells (DSSCs). XRD and FE-SEM were used to analyze the crystal structure and morphological properties of the produced TiO_2 nanopowders, respectively. The optical properties of natural dyes extracted from the *Salvia urica* plant were investigated by UV-vis spectroscopy. Functional groups in natural dyes were detected by FTIR spectroscopy, while DSSCs were evaluated for photovoltaic performance and electrochemical impedance. The findings confirmed that the dye obtained from the flower absorbs a wider wavelength of light in the visible region. Among all other natural sensitizers, the highest power conversion efficiency was seen in the flower dye-sensitized cell. This situation was explained by the very strong interaction of the carboxyl/hydroxyl groups and the TiO_2 surface. The efficiencies of DSSCs sensitized with flower, branch and leaf dye of *Salvia urica* were 0.33%, 0.28%, and 0.19%, respectively.

## *Salvia urica*'nın Farklı Kısımlarından Ekstrakte Edilen Boyaların Boya Duyarlı Güneş Pillerinde Kullanımı

Öz: Bu çalışmada TiO_2 esaslı boya duyarlı güneş pillerinde hassaslaştırıcı olarak *Salvia urica*'nın yapraklarından, çiçeklerinden ve dallarından faydalanıldı. Sentezlenen TiO_2 nano tozlarının kristal yapısını ve morfolojik özelliklerini analiz etmek için sırasıyla XRD ve FE-SEM kullanıldı. *Salvia urica* bitkisinden ekstrakte edilen doğal boyaların optik özellikleri UV-vis spektroskopisiyle incelendi. Boya duyarlı güneş pilleri fotovoltaik performans ve elektrokimyasal empedans açısından incelenirken doğal boyalardaki fonksiyonel gruplar FTIR spektroskopisiyle tespit edildi. Bulgular, çiçekten elde edilen boyanın görünür bölgede ışığı daha geniş bir dalga boyunda absorbe ettiğini doğruladı. Diğer tüm doğal hassaslaştırıcılar arasında en yüksek güç dönüşüm verimi çiçek boyasıyla duyarlılaştırılmış hücrede görüldü. Bu durum karboksil/hidroksil grupları ile TiO_2 yüzeyinin çok güçlü etkileşimi ile açıklandı. *Salvia urica*'nın çiçek, dal ve yaprak boyası ile duyarlı hale getirilen DSSC'lerin verimliliği sırasıyla % 0,33, % 0,28 ve % 0,19 bulundu.

1. INTRODUCTION

Rapidly increasing industrialization brings energy demands to higher levels [1]. All countries have turned to alternative energy sources for meeting their increasing energy demands [2]. One of the main causes of this is that fossil fuels will run out shortly and pose a risk to the environment [3]. This viewpoint emphasizes how important environmentally friendly and renewable

sources of energy are [4]. Particularly alluring are photovoltaic systems, which directly transform solar energy through electrical power [5]. Due to their high efficiency, solar cells made with silicon achieved an important milestone on the path to commercialization in these circumstances [6]. Many developed and developing countries use these silicon-based photovoltaic modules extensively and produce energy. However, as silicon-based solar cells are costly, studies on eco-friendlier and

more economical solar cell technologies have accelerated [7]. Thanks to their low cost and easy production processes, dye-sensitized solar cells are pivotal to scientific and technological developments within this framework [8]. As a result of intensive studies on DSSCs, power conversion efficiencies of over 15% have been achieved [9]. This is an important step toward the commercialization of DSSCs in a short span time [10]. Researchers are attempting to improve the power conversion performance of DSSCs by focusing on the photonode layer, dye, redox electrolyte, and counter electrode because the efficiency of these devices is still below the level that is desired [11]. The components of a DSSC are a dye molecule, counter electrode, electrolyte solution, and photoanode layer [12]. The mechanism of operation of a typical DSSC seems quite simple, as shown in Fig. 1. Sensitizing molecules of dye absorb the photon flux emitted on the exterior of TiO_2 when light strikes the photoanode layer, exciting the electrons in the sensitizer [13]. The transparent conductive oxide, the electrolyte solution, and the cathode, in that order, receive the generated current. In order to finish the cycle and direct the ions into the dye solution, the counter electrode provides ions into the redox solution.
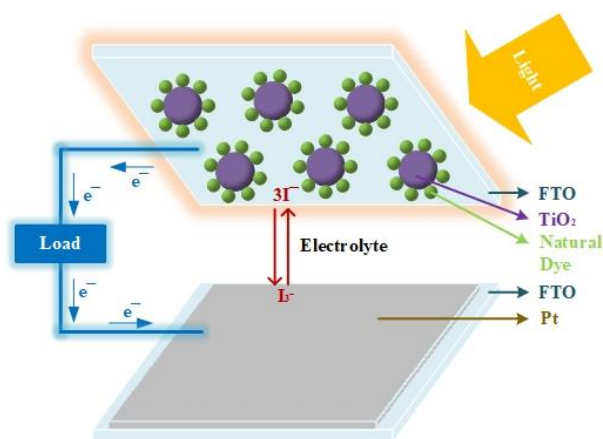
Figure 1. A standard DSSC's operating concept.

There are two types of dyes employed in DSSCs: natural and synthetic. Synthetic dyes are also categorized as metal-free organic dyes and metal complex dyes [14]. The classification of dyes used as sensitizers in DSSCs is given in Fig. 2. The dye used as a sensitizer in DSSCs is important for photovoltaic performance. The properties that the dye used in a DSSC must have are summarized below [15];

- Its visible region must possess a strong absorption quality.
- It must contain carbonyl and/or hydroxyl groups that will create energetic interaction with the TiO_2 surface.
- The lowest conduction band must match the Lowest Unoccupied Molecular Orbital (LUMO) level.
- The redox level of the electrolyte solution must be higher than the Highest Molecular Orbital (HOMO) level.

Metal complex dyes have been utilized in DSSCs to achieve high power conversion efficiencies. In particular, DSSCs with power conversion efficiencies over 15% have been successfully produced using Ruthenium (Ru) based dyes [16]. On the other hand, these dyes are expensive and pose a great risk to the environment. Additionally, metal complex dyes face stability problems due to recombination events within the cell [17]. This circumstance has brought attention to metal-free organic dyes, which are an excellent substitute because they are less harmful to the environment, affordable, readily accessible, and do not contain metal. Intensive research has been conducted to achieve high power conversion efficiency in DSSCs using metal-free organic dyes [18]. Metal-containing dyes have lower extinction coefficients than metal-free organic-based dyes. Additionally, they enable the use of thinner oxide films that minimize energy losses during charge transfer [19]. However, because of their intense and narrowed absorptions in the visible light spectrum's blue region, they have a low light collection efficiency. In this instance, the metal-free organic dye-sensitized DSSCs' efficiency values stayed below 10% [20].

The high costs of metal complex dyes, difficult synthesis steps and environmental hazards limit the wide range of use of these dyes in DSSCs and encourage the search for alternative sensitizers. This makes the non-toxic, environmentally friendly natural sensitizing dyes prominent [13]. Numerous organic dyes have already been investigated thus far for use as DSSC sensitizers. Among these dyes, the most commonly used are chlorophylls, carotenoids, betalains, anthocyanins and flavonoids [21]. The classification of natural dyes is determined by the chemical structures and photophysical properties of plants. Carbonyl and/or hydroxyl groups in the plant structure have a strong interaction with the TiO_2 surface due to their chemical structure [22]. This kind of interaction lessens the recombination of charge in the contact point and promotes electron transfer to TiO_2's conduction band [23]. Natural dyes obtained from plants are put to use in areas such as the pharmaceutical industry, textile dyes and food [24]. Among these plants, the genus *Salvia* has an important place in the food, medicine and cosmetic industries. *Salvia urica*, also known as lime tea, grows in the Mediterranean region and is in high demand due to its aromatic properties. Dyes extracted from the above-ground parts of the *Salvia urica* plant have antibacterial, antifungal and dyeing properties [25]. The main pigment found in the structure of this plant is eupatilin and they are organic compounds defined as 6-0-methylated flavonoids. Eupatilin is considered a flavonoid as it represents the methoxy groups of the C6 atom attached to the flavonoid backbone [26]. Nonetheless, DSSCs sensitized with natural dyes do not possess the desired level of power conversion efficiency, so researchers have carried out different studies to increase the stability of the dyes used in DSSCs. Researchers have implemented strategies such as purification by column chromatography [27], the use of different extraction methods [28], and mixing natural dyes [29]. In a study by Zhou et al., catalysts in DSSCs were made from natural dyes that were taken from 20 various plants, and the highest efficiency value (1.17%) was obtained from *Mangosteen* extract [30]. In a study by Kristoffersen et al., cell performance increased significantly after the removal of nonpigmentary organic

162

components from the anthocyanin dye [31]. In a study reported by Hamadanian et al., the cell sensitized with the *Consolida ajacis* plant exhibited the highest cell performance with 0.6% among 10 different plant extracts [32]. In a study by Ramomoorthy et al., cells sensitized with a mixture of betalain and anthocyanin showed the highest efficiency [33]. Nnorom et al., obtained the highest power conversion efficiency (0.58%) by using *Baphia nitida* dye in DSSCs prepared using natural sensitizers [3]. In a study by Calogero et al., cell efficiency was improved by up to 1.6% by using different extraction methods [34]. Ahmadi et al improved the filling factor up to 0.76 in lichen *Collema nigra* dye-sensitized DSSCs [35]. Singh et al. reported 0.72 mA/cm^2 J$_{sc}$, 5.55 V V$_{oc}$, 0.70 FF and 0.28% power conversion efficiency using *Tropaeolum majus* flowers as sensitizers [36]. When the studies conducted with natural dyes are examined, attempts have been made to increase the power conversion efficiency of DSSCs by using techniques such as different dye extraction methods, different solvents, purification processes and mixing natural dyes. The aim of this study is to investigate how dyes extracted from different parts of a plant species that have not previously been used in DSSCs affect cell performance.

Three DSSCs were made for this study using dyes that were extracted from the *Salvia urica* plant's leaves, branches, and flowers. DSSCs sensitized with *Salvia urica* have not been previously reported in the literature. It has also been observed that natural dyes that were gleaned from various sections of the plant have different sensitization performance.
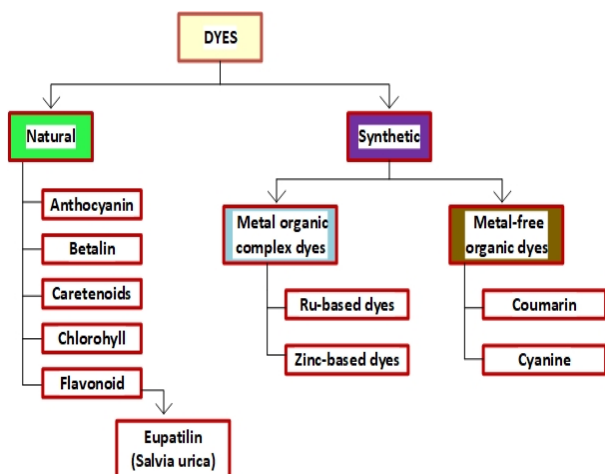
Figure 2. Classification of dyes used as sensitizers in DSSCs.

2. EXPERIMENTAL

2.1. Materials

The *Salvia urica* plant used as a sensitizer in this study was obtained from the city of Elazig in the Eastern Anatolia Region of Turkey. The chemicals were purchased commercially to be used in the experiments and they were not subjected to additional purification. The chemicals used in the study and the companies from which they were purchased are summarized below;

- Tetraisopropyl (TTIP)- ≥97.0% purity – Acros Organic
- Ethyl cellulose - Sigma-Aldrich

- α-terpineol - Acros Organic
- FTO glass-TC030 sodalime/resistivity10 Ω/sq-Solaronix
- Pt Pastes (Liquit paint:Platisol-T)-Aldrich
- Redox solution (AN-50) - iodide/tri-iodide/Solaronix
- Thermoplastic sealing gasket (Meltonix 20 µm)/Solaronix
- Absolute ethanol (ethyl alcohol)- Sigma-Aldrich
- Hydrochloric acid (HCl) - Sigma-Aldrich.

2.2. Synthesis of TiO₂ Nanoparticles

In this study, TiO$_2$ based nanopowders were synthesized by the sol-gel method that was also used previously [37]. 2 ml TTIP and 50 ml absolute ethanol were mixed vigorously at ambient temperature until the color of the mixture turned yellow. While this process was continuing, 0.19 ml HCl was added dropwise to the mixture and stirred for another 24 h. Pure water and alcohol were used several times to wash the precipitate obtained after centrifugation. The cleaned precipitate was kept in an oven at 50 °C to dry for 12 h before it was sintered in a high temperature operate furnace at 400 °C for 1 h. The synthesized TiO$_2$ particles were pulverized with a mortar and stored in a desiccator in a dark environment.

2.3. Extraction of Natural Dyes

The leaves, branches and flowers of the *Salvia urica* plant were carefully removed from the plant skeleton. Plant parts were cleaned of dust by repeatedly washing leaves and branches in pure water and then drying them in an oven. These plant parts were pulverized with the help of a high-speed grinder. A 10 g portion of each powder was placed into 3 different soxhlet cartridges. Each soxhlet system received ethyl alcohol (150 ml) and the system was siphoned until the dye extraction was finished. In this study, ethyl alcohol was used as a solvent to separate the dye from plants. Many previous studies have shown that eupatilin dye is more soluble in ethyl alcohol [32,38,39]. The extracted dyes were adjusted to the appropriate concentration with the help of a rotary evaporator so that 80% of the alcohol was recovered. Finally, it was passed through a filter paper to remove insoluble residues in the dye and stored in a dark environment at 4 °C. In Fig. 3, the extraction processes of natural dyes are shown.

163
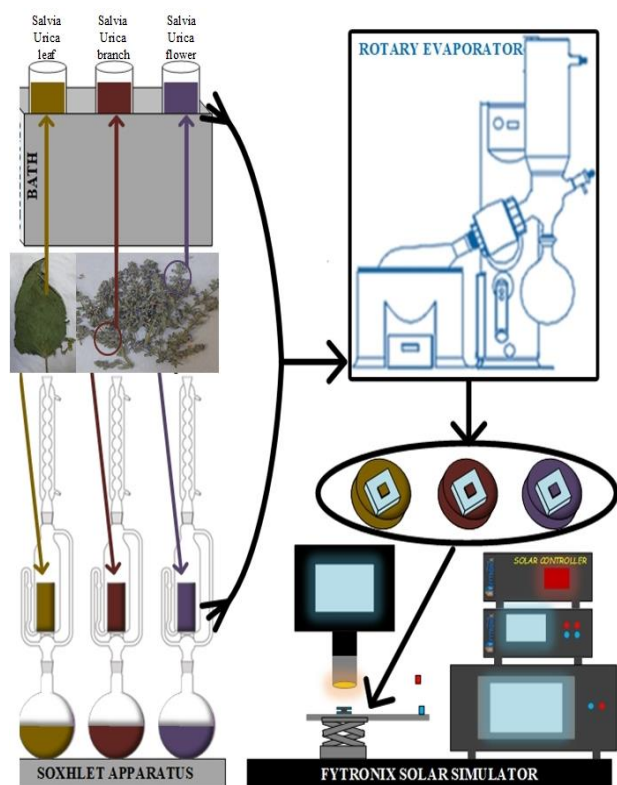
Figure 3. Extraction of dye from flowers, branches and leaves of *Salvia urica*.

2.4. Assembling of DSSC

TiO$_2$ paste was prepared with the same procedure that was used in previous studies on high-performance DSSCs [40]. For this purpose, 225 mg TiO$_2$, 100 mg ethyl cellulose and 10 ml absolute ethanol were ultrasonically mixed until the dispersion of TiO$_2$ particles in the mixture. After the ultrasonic treatment was completed, this mixture was magnetically stirred strongly (1000 rpm) for 24 h in a dark environment at room temperature. Some of the alcohol in the mixture was removed with the help of a rotary evaporator to achieve the appropriate paste consistency. Then, the process of cleaning the FTO was started. Commercially purchased FTO glasses were ultrasonically treated separately in acetone, ethyl alcohol and water. Using the doctor blade method, a synthesized paste was created on the conductive part of the cleaned glasses. The produced photoelectrodes were sintered for 45 min at 450 °C after being dried in an oven for 30 min at 80 °C. The photoelectrodes were left in a vacuum desiccator to cool following the sintering process. The preparation stages of the photoanode layer are given in Fig. 4. When the temperature of the photoelectrodes dropped to an average of 70 °C, they were removed from the desiccator. While the TiO$_2$ thin film was in the up position, it was dipped into previously prepared natural dyes and left for 24 h. Photoanodes sensitized with natural dyes were immersed in an alcohol solution several times to remove undissolved residues on the TiO$_2$ surface. These photoanodes, sensitized with natural dyes, were quickly dried in the cold air form of a dryer and stored in a desiccator. After the preparation of the photoanode layer, the production of Platinum (Pt) counter electrodes began. The even distribution of the commercially purchased platisol paste on the conductive part of the pre-

cleaned FTO was handled with an acrylic brush. The Pt paste was spread smoothly on the conductive part of the FTO with a brush and heat treated at 450 C for 15 min. For the assembly of DSSCs, a thermoplastic seal was placed around the TiO$_2$ thin films and combined with the counter electrode. To combine the sealing gasket and the counter electrode, the photoanode layer was subjected to heat treatment at 100 °C for 20 s. Redox solution was injected onto the TiO$_2$ surface through a hole on the upper surface of the Pt electrode, using a special syringe that prevents the formation of air gap.
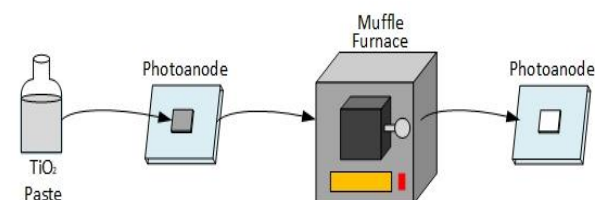
Figure 4. Preparation of the photoanode layer.

The production of DSSCs was completed after a thermoplastic sealing gasket was utilized to close the hole in the Pt electrode. A representative view of a typical DSSC is seen in Fig. 5.
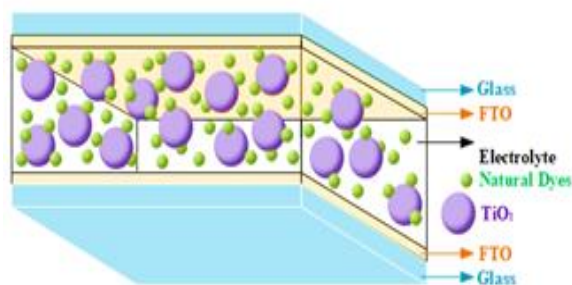
Figure 5. Parts of a consolidated DSSC.

2.5. Characterization

In this study, the crystal structure and morphological properties of TiO$_2$ thin films produced by the sol-gel method were analyzed with the Rigaku X-ray diffraction (XRD) system and Zeiss Sigma 300 field emission electron microscope (FESEM), respectively. While the measurement of the thickness of TiO$_2$ films was carried out with Kla Stylus Profiler P7, Brunauer-Emmett-Teller (BET) was used to determine the pore size and specific surface area of the synthesized TiO$_2$ particles. The absorption properties of the extracted natural dyes were measured with the UV-3600 Shimadzu-Japan device. Fourier transmission infrared (FTIR) spectra were used to detect some functional groups in natural dyes (Thermo Scientific Nicolet Summit device). Electrochemical Impedance Spectra (EIS) and Photovoltaic measurements of DSSCs were recorded by the Fytronix Impedance Analysis System and the LSS 9000 I-V Characterization System (Fytronix Solar Simulator).

164

3. RESULTS AND DISCUSSION

The method called sol-gel is employed to produce TiO$_2$ nanoparticles which structures can be ssen in Fig. 6. The sharp peaks seen in the Fig. 6 reflect the crystalline nature of TiO$_2$ nanoparticles. The peak positions (101) (004) (200) (105) (211) (204) (116) (220) (215) correspond to the anatase TiO$_2$ according to JCPDS card number: 50-00-223. The photoanode layer in high-performance DSSCs is mostly formed with anatase TiO$_2$ [41].

The average particle size of the metal oxide semiconductor TiO$_2$ nanopowder was determined using the William-Son-Hall formula and XRD spectra seen in the Eq. 2[42]. βs in this equation reflects the FWHM, which is the full-width value at half the height of the peak. The symbols "ε", "θ", "D", and "ʎ" in the equation correspond to the lattice voltage, reflection angle of the peaks, crystal size, and X-ray wavelength, respectively. The average crystal size of TiO$_2$ particles synthesized according to this formula is 14.28 nm.

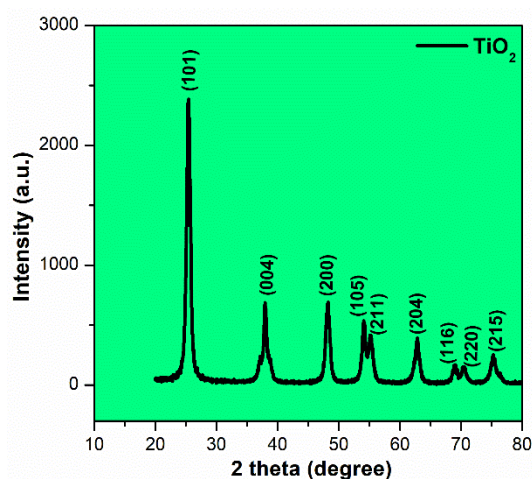$$\beta \cos \theta = \frac{0.9\lambda}{D} + 4\varepsilon \sin \theta \qquad (1)$$

Figure 6. XRD example of the synthesized metal-oxide semiconductor nanopowder.

Fig. 7 shows the surface photographs of the TiO$_2$ thin film coated on the FTO surface using the doctor blade method at 1 μm and 100 nm scales. As seen in the Fig.7, almost all TiO$_2$ nanoparticles have a spherical structure. TiO$_2$ nanoparticles are tightly bonded to each other. The tight contact of thousands of aggregations improves electron transport. Such a contact provides more pathways for the transport of electrons injected into the thin film and minimizes electron losses [43]. The average size of TiO$_2$ nanoparticles in the photoanode layer is 15 nm. Nanoparticles have a central function as donors and acceptors in the active layer of DSSCs. The size of TiO$_2$ nanoparticles in the photoanode layer affects both electron transfer and recombination states of holes. As the size of the particles decreases, the surface/volume ratio and surface area increase. This causes increased dye absorption on the surface [44].
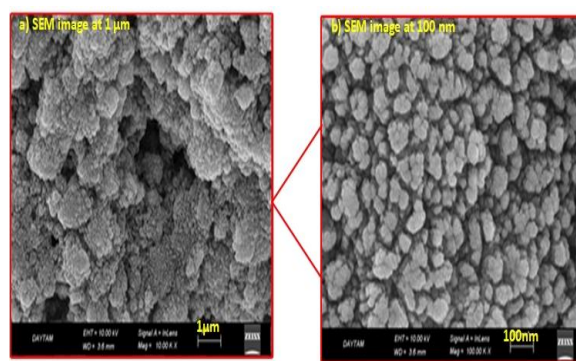

Figure 7. SEM images at different scales of TiO2 based nanopowder produced with the sol-gel technique.

The specific surface area and pore size of the produced TiO$_2$ nanopowders were determined by the BET method. The isotherm curve of the produced sample is given in Fig. 8. The adsorption and desorption curves of N$_2$ gas are associated with the Brunauere Deminge Deminge Teller (BDDT) classification. According to this classification, the synthesized TiO$_2$ particles reflect the isotherm type IV and mesoporous structure. Both pore size and specific surface area of TiO$_2$ in DSSCs play important roles in cell performance. The specific surface area and pore size of the synthesized TiO$_2$ particles were recorded as 6.28 m^2/g and 70.95 nm, respectively. Increasing the specific surface area and pore size of nanoparticles in the photoanode layer improves the dye loading and electron transport pathways of the TiO$_2$ thin film [45]. Morphological parameters obtained from BET studies showed that the synthesized TiO$_2$ nanoparticles were suitable for high-performance DSSCs [46].
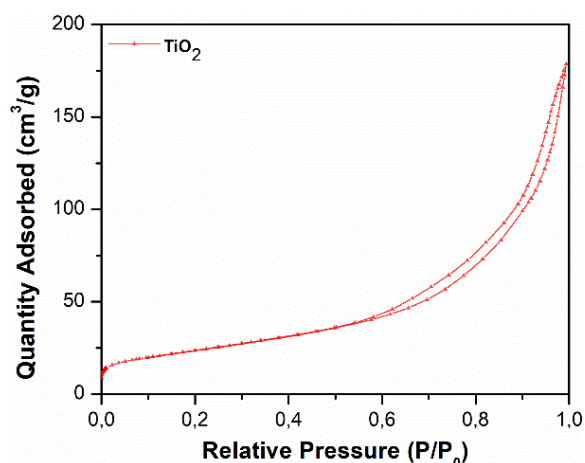
Figure 8. N$_2$ adsorption/desorption graphs of semiconductor metal-oxide TiO$_2$ powders.

Fig. 9 shows the UV–vis absorption spectra of dyes obtained via flowers, *Salvia urica* plant' branches and leaves. Such dyes can evidently be used as sensitizers in DSSCs, for light is absorbed by them in the UV-vis. Differences in the absorption behavior of the dyes significantly affected the performance of the synthesized solar devices. This is due to the different pigment structures in natural dyes. The maximum absorbance wavelength of 3 dyes extracted from different sections of the *Salvia urica* plant is 660 nm. Additionally, the dye extracted from the flower has an additional peak at 473 nm. The dye utilized by the plant's flowers exhibits two

distinct peak patterns inside the visible region, indicating that it has the highest absorption. Peaks at 660 nm indicate that the dye is eupatilin, which generally belongs to the flavonoid class [32]. The extra peak exhibited by the flower dye at 473 nm reveals the presence of chlorophyll in the respective dye extract. Chlorophyll is known to strongly absorb light within the observable spectrum, particularly from wavelengths as 400 to 500 nm [47]. Compared to dyes extracted from the branches and leaves, the Salvia urica plant's flowers demonstrated absorption at a wider wavelength in the visible spectrum. It is known that the absorption behavior at this wider wavelength increases cell performance [48]. Additionally, absorptions in different energy regions help DSSCs capture more photons [49]. The dye obtained from the flowers of the *Salvia urica* plant absorbs a wider wavelength, resulting in higher cell performance. Furthermore, dyes obtained from various plant parts may have different absorption qualities, according to UV research.
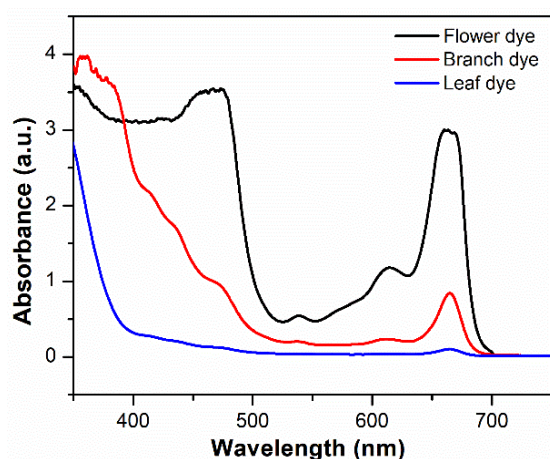

Figure 9. Natural dye absorption spectra obtained from various components of Salvia urica.

Fig. 10 shows the FTIR spectra of 3 natural dyes leached from different sections of the *Salvia urica* plant. The chemical structure of eupatilin, the basic pigment of *Salvia urica*, is given in Fig. 11. The functional groups that constitute the basic structure of natural dyes that are put to use as sensitizers in cells were determined thanks to the spectrum which shown at the Fig. 10. For natural dyes to form a strong interaction with the TiO_2 surface, they must contain carbonyl and/or hydroxyl groups in their chemical structure. Natural dyes that are derived from various sections of the plant showed identical spectral properties, and the presence of functional groups in the main pigments is manifested by the peaks observed in the IR spectra of these dyes [14,32,47]. However, the spectrum of the dye derived from the flowers of the *Salvia urica* plant showed stronger characteristic absorption. This is due to the superposition of the two main pigments (chlorophyll, and eupatilin) in the dye [38]. The dyes obtained from this plant's branches and leaves have nearly identical spectra. The hydroxyl group presence in the three natural dye extracts is indicated by the broad peak at 3321 cm^{-1} [50]. The peaks at 2923 and 2851 cm^{-1} are attributed to alkyl C-H of polyphenolic compounds [14,48]. The peaks appearing at 1600 cm^{-1} correspond to aromatic ring vibrations [49]. The peak at 1259 cm^{-1} is assigned to the C-N stretching of amine groups, while the

sharp peak observed at 1046 cm^{-1} corresponds to the C-O-C stretching of carbohydrate or ester groups [3,21]. The bands attributed to 990 and 917 cm^{-1} arise from out-of-plane bendings of the C-H bond [51]. FTIR test results clearly show that, for DSSCs, natural pigments containing carbonyl and/or hydroxyl functional groups are applicable and useful sensitizers.
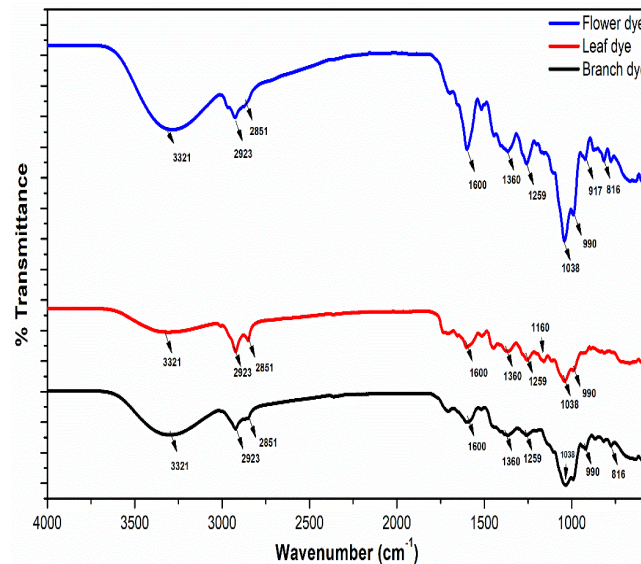
Figure 10. FTIR spectra of dyes leached from flowers, branches and leaves of the Salvia urica plant.
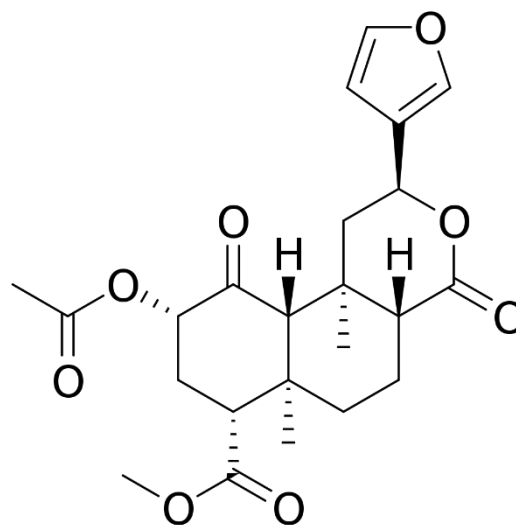
Figure 11. Chemical structure of eupatilin.

The electrochemical impedance spectra (EIS) of DSSCs sensitized with natural dyes are shown in Fig. 12(a). Under 100 mW/cm2 of enlightenment, EIS analyses were recorded in frequency ranges ranging from 0.1 Hz to 100 kHz. With the aid of the Zview program, resistance parameters were computed from EIS data and are shown in Table 1. DSSC electrochemical spectra are typically shown as three semicircles. There is a correspondence between the first semicircle in the high-frequency region and the charge transfer at the counter electrode. The back reaction at the TiO_2/electrolyte interface and the transport of injected electrons in the TiO_2 film are mirrored by the second semicircle in the mid-frequency region. The third semicircle in the low-frequency region is attributed to the Warburg diffusion process of I$^-$/I$_3^-$ in the redox electrolyte

166

[52]. In the Nyquist diagram shown in Fig. 12(a), semicircles of the high and medium-frequency regions can be seen. The absence of the third semicircle in the low-frequency region may be due to Warburg diffusion of redox couples [53]. The series resistance (R_s) value is associated with the intersection of the high-frequency region with the real axis, while R_{ct1} and R_{ct2} stand for the resistance of the charge transfer at the electrode as Pt and the resistance of electron transfer between TiO_2-electrolyte, respectively. It can be seen in Table 1 that R_s and R_{ct1} values are very close to each other since the same Pt electrode and iodide/tri-iodide redox solution were used in DSSCs sensitized with natural dyes [54]. Therefore, when examining the interface resistances of cells, the impedance value (R_{ct2}) that originates from the transfer of electron out of the conduction band of TiO_2 to the FTO glass must be taken as the reference. Increasing the diameter of the Nyquist curves representing R_{ct2} leads to lower cell performance. When Table 1 is examined, the R_{ct2} values of DSSCs sensitized with the flower, branch and leaf dye of the plant were calculated as 120.6, 140.1 and 162.7 Ω, respectively. DSSCs sensitized with sensitizers obtained from the branches and leaves of the *Salvia urica* plant have higher R_{ct2}. The higher charge transfer resistances of these cells cause higher distortion and separation and negatively affect their power conversion efficiency [55]. In addition, due to increasing R_{ct2} values, the V_{oc} values of the DSSCs produced decreased from 0.65 to 0.55 V. Because as the R_{ct2} value increases, slower electron transfer occurs at the TiO_2/electrolyte interface, resulting in lower V_{oc} values [56]. In DSSCs, low R_{ct2} values accelerate the charge transfer between the photoanode layer and the Pt electrode. The lower R_{ct2} value shown by flower dye-sensitized DSSC is consistent with the higher cell performance it exhibits [57].

Table 1. EIS parameters of DSSCs sensitized with flowers, branches and leaves of *Salvia urica*.

Sample	R_s (Ω)	R_{ct1} (Ω)	R_{ct2} (Ω)	C_e (μs)
DSSC sensitized with flowers of *Salvia urica* plant	15.3	6.4	120.6	1310
DSSC sensitized with branches of *Salvia urica* plant	17.1	8.1	140.1	834
DSSC sensitized with leaves of *Salvia urica* plant	19.2	8.9	162.7	752

Electron lifetimes (C_e) of DSSCs obtained via natural dyes acquired from different Salvia urica plant sections were calculated with the help of Eq. 2 [58] from the Bode graph given in Fig. 12(b). The fmax in Eq. 2 is the maximum peak frequency of the Bode lines. The C_e values of DSSCs sensitized with flower, branch and leaf dye were found to be 1310, 834 and 752 µs, respectively. The higher electron lifetime of flower dye-sensitized DSSC is due to its higher recombination resistance. Increasing electron lifetime in a cell improves cell performance by limiting the recombination of electrons and redox pairs [59]. Conversely, though the f_{max} value of DSSC obtained via dye leached from the leaves of *Salvia urica* has the lowest electron lifetime since it is in the

high-frequency region. This caused the leaf-sensitized cell to have the lowest efficiency value.

$$\tau_e = \frac{1}{2\pi f_{(max)}} \qquad (2)$$
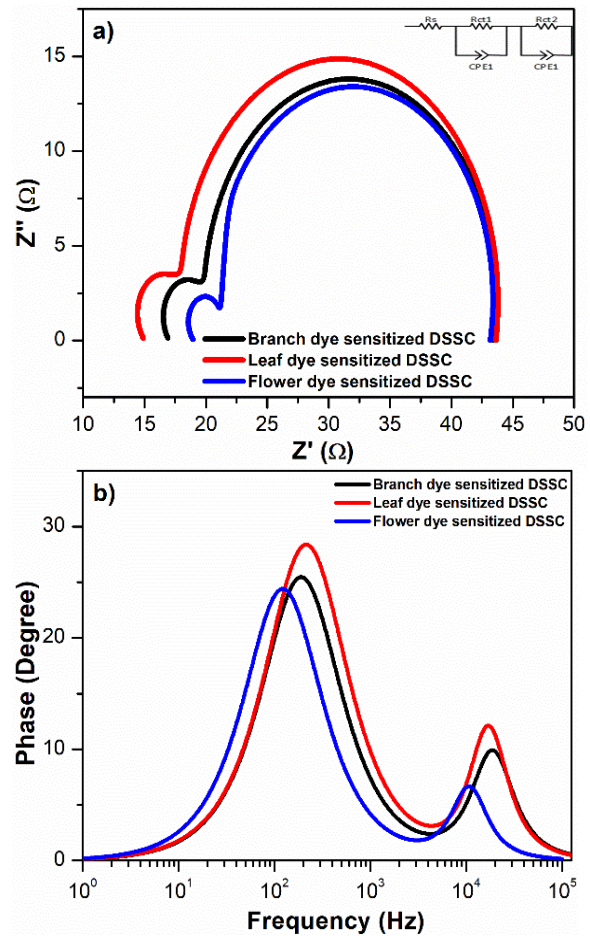
Figure 12. a) Nyquist curves, **b)** Bode curves of DSSCs using sensitizers extracted from different parts of *Salvia urica*.

Photoelectric properties of DSSCs sensitized with flower, branch and leaf dye of the *Salvia urica* plant were examined using artificial sunlight under 100 mW/cm^2 light intensity (AM 1.5G). J_{sc}-V curves of DSSCs sensitized with natural dyes are seen in Fig. 13. Photovoltaic cell parameters for instance efficiency of cell (Ƞ), density of short circuit (J_{sc}) current, open circuit (V_{oc}) voltage and factor of filling (FF) of natural dyes based DSSCs were calculated by Eq. 3, 4 as is shown in Table 2. Compared with other sensitizers, the flower dye-sensitized cell has the best cell efficiency (Ƞ= 0.33) with a short-circuit current density of 0.73 mA/cm^2, an open-circuit voltage of 0.65 V, and a filling factor of 0.71. When DSSCs sensitized with dyes leached from different parts of the *Salvia urica* plant are compared to the performance of cells produced with conventional inorganic Ruthenium complex dyes (Ƞ=6.86%), the cell efficiency is very low [13]. However, intensive research on organic-based dyes shows that these dyes are promising for DSSCs in the near future [60]. Additionally, in a study reported

167

by Lohar et al., they reported a cell performance of 0.152 % in cells where *Salvia divinorum*, one of the different species of *Salvia*, was used as a sensitizer. The photoelectric performance of DSSC sensitized with dye obtained from the flowers of the *Salvia urica* plant is higher than cells sensitized with branch and leaf dye. This may be due to the higher presence of some functional groups that show superior performance in DSSCs in the flower-extracted dye. Because the charge transfer transition of flavonoid and chlorophyll pigments from HOMO to LUMO requires less energy. As a result of such behavior, the pigment molecules are energized by visible light, resulting in a wider absorption band in the UV-vis [61]. Two intense absorptions of the flower dye over a wide area in the visible region support this situation. Moreover, the higher V_{oc} value (0.65 V) of DSSC sensitized with flower dye is a result of the strong interaction of alkyl chains with the TiO_2 surface. Such an interaction prevents the leakage of electrons from the photoanode layer into the electrolyte solution [62]. The lower V_{oc} (0.55 V) and J_{sc} (0.52 mA/cm²) values of the leaf dye-sensitized cell can be attributed to the poor electron injection and the low concentration of some pigments that exhibit high performance in DSSCs [63]. As a result, it appears that dyes leached from different parts of natural plants may have different sensitization performances.

$$\eta = \frac{P_{max}}{P_{in}} = \frac{V_{oc} \times J_{sc} \times FF}{P_{in}} \qquad (3)$$

$$FF = \frac{J_{max} \times V_{max}}{J_{sc} \times V_{oc}} \times 100 \qquad (4)$$
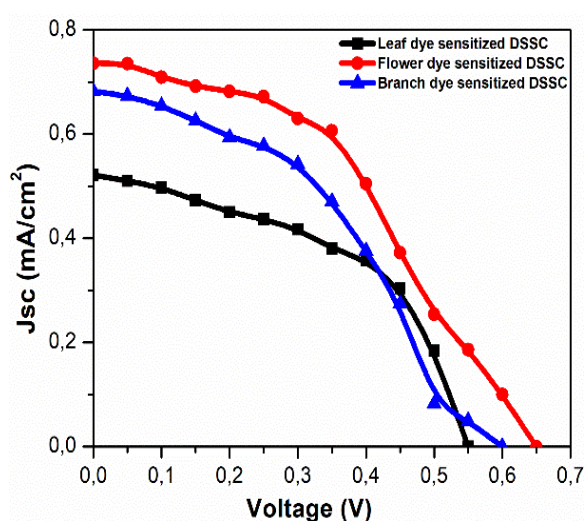

Figure 13. The DSSCs' Jsc-V curves sensitized with dyes of the Salvia urica plant's flowers, leaves and branches.

Table 2. DSSCs' photovoltaic results sensitized with flowers, branches and leaves of *Salvia urica*.

Sample	J_{sc} (mA/cm²)	V_{oc} (V)	FF	η (%)
DSSC sensitized with flowers of *Salvia urica* plant	0.73	0.65	0.71	0.33
DSSC sensitized with branches of *Salvia urica* plant	0.68	0.60	0.69	0.28
DSSC sensitized with leaves of *Salvia urica* plant	0.52	0.55	0.68	0.19

4. CONCLUSION

In this study, the performance of dyes extracted from the flowers, branches and leaves of the *Salvia urica* plant on DSSCs was examined. The production of TiO_2 nanoparticles was successfully performed using the sol-gel method and photoelectrodes were prepared by the doctor blade method. XRD studies confirmed that TiO_2 was in the anatase phase. SEM images showed that TiO_2 nanoparticles had a spherical structure in close contact with each other. Fourier spectroscopy testing revealed that dyes containing carbonyl and hydroxyl groups were suitable sensitizers for DSSCs. Dyes extracted from the flowers, branches and leaves of the *Salvia urica* plant showed different absorption behaviors in the visible region. UV-vis studies showed that the flower dye exhibited absorption over a wider wavelength range in the visible region. It was determined from EIS analysis that the longest electron lifetime (1310 ms) was in the flower dye-sensitive DDSC. This was attributed to the high recombination resistance of the flower dye-sensitized cell. The flower dye-sensitized DSSC exhibited the best cell performance (0.33%) with, 0.71 FF, 0.65 V V_{oc} and 0.73 mA/cm² J_{sc}. This behavior was explained by the strong absorption of the flower dye in the visible region and the higher presence of some functional groups in this natural dye. The low V_{oc} (0.55 V) and J_{sc} (0.52 mA/cm²) values of the leaf dye-sensitized cell were attributed to poor electron injection and low concentration of some high-performance pigments. Dyes extracted from different parts of natural plants may exhibit different sensitizing performances in DSSCs. In addition, natural dyes used as sensitizers in DSSCs can offer a sustainable solution to meet energy needs as they are cheaper and eco-friendly. The use of dyes to be leached from different parts of plants with different extraction methods in DSSCs is promising for high-performance DSSCs. Organic-based dyes, especially those obtained with pure critical and high-pressure extraction systems, can be used as high-performance sensitizers in DSSCs.

168

REFERENCES

[1] Kumar BA, Vetrivelan V, Ramalingam G, Manikandan A, Viswanathan S, Boomi P, Ravi G. Computational studies and experimental fabrication of DSSC device assembly on 2D-layered TiO2 and MoS2@TiO2 nanomaterials. Physica B: Condensed Matter. 2022;633: 413770.

[2] Katta VS, Chappidi VR, Kumar A, Asthana S, Raavi SSK. Enriched visible light absorption by Au-embedded Sm3+ doped TiO2 compact photoanode for enhanced dye-sensitized solar cell performance. Physica B: Condensed Matter. 2023;652:414621.

[3] Nnorom OO, Onuegbu GC, Etus C. Photo-performance characteristics of Baphia nitida and rosella dye sensitized solar cell. Results in Optics. 2022;9:100311.

[4] Akman E. Enhanced photovoltaic performance and stability of dye-sensitized solar cells by utilizing manganese-doped ZnO photoanode with europium compact layer. Journal of Molecular Liquids. 2020;317:14-22.

[5] Zatirostami A. A dramatic improvement in the efficiency of TiO2-based DSSCs by simultaneous incorporation of Cu and Se into its lattice. Optical Materials. 2021;117:111110.

[6] Hadi A, Alhabradi M, Chen Q, Liu H, Guo W, Curioni M, Cernik R, Liu Z. Rapid fabrication of mesoporous TiO 2 thin films by pulsed fibre laser for dye sensitized solar cells. Applied Surface Science. 2018;428:1089–1097.

[7] Xu J, Wang G, Fan J, Liu B, Cao S, Yu J. G-C3N4 modified TiO2 nanosheets with enhanced photoelectric conversion efficiency in dye-sensitized solar cells. Journal of Power Sources. 2015;274:77–84.

[8] Wang Z, Fang J, Mi Y, Zhu X, Ren H, Liu X, Yan Y. Enhanced performance of perovskite solar cells by ultraviolet-ozone treatment of mesoporous TiO 2. Applied Surface Science. 2018;436:596–602.

[9] Kakiage K, Aoyama Y, Yano T, Oya K, Fujisawa JI, Hanaya M. Highly-efficient dye-sensitized solar cells with collaborative sensitization by silyl-anchor and carboxy-anchor dyes. Chemical Communications. 2015;51:15894–15897.

[10] Xie Y, Huang N, You S, Liu Y, Sebo B, Liang L, Fang X, Liu W, Guo S, Zhao XZ. Improved performance of dye-sensitized solar cells by trace amount Cr-doped TiO2 photoelectrodes. Journal of Power Sources. 2013;224:168–173.

[11] Zatirostami A. Electro-deposited SnSe on ITO: A low-cost and high-performance counter electrode for DSSCs. Journal of Alloys and Compounds. 2020;844:156151.

[12] Chu L, Qin Z, Zhang Q, Chen W, Yeng J, Yang J, Li X. Mesoporous anatase TiO 2 microspheres with interconnected nanoparticles delivering enhanced dye-loading and charge transport for efficient dye-sensitized solar cells. Applied Surface Science. 2016;360:634–640.

[13] Akman E, Karapinar HS. Electrochemically stable, cost-effective and facile produced selenium@activated carbon composite counter electrodes for dye-sensitized solar cells. Solar Energy. 2022;234:368–376.

[14] Ammar AM, Mohamed HSH, Yousef MMK, Abdel-Hafez GM, Hassanien AS, Khalil ASG. Dye-Sensitized Solar Cells (DSSCs) based on extracted natural dyes. Journal of Nanomaterials. 2019;186:172-186.

[15] Ludin NA, Al-Alwani A.M, Bakar A, Kadhum AA, Sopian K, Abdul Karim NS. Review on the development of natural dye photosensitizer for dye-sensitized solar cells. Renewable and Sustainable Energy Reviews. 2014;31:386–396.

[16] Al-Alwani MAM, Ludin NA, Mohamad AB, Kadhum AAH, Mukhlus A. Application of dyes extracted from Alternanthera dentata leaves and Musa acuminata bracts as natural sensitizers for dye-sensitized solar cells. Spectrochimica Acta - Part A: Molecular and Biomolecular Spectroscopy. 2018;192:487–498.

[17] Kumara NT, Petrović M, Peiris DS, Marie YA, Vijila C, Petra MI, Chandrakanth, RL, Lim CM, Hobley J, Ekanayake P. Efficiency enhancement of Ixora floral dye sensitized solar cell by diminishing the pigments interactions. Solar Energy. 2015;117:36–45.

[18] Omar A, Ali MS, Rahim N. Electron transport properties analysis of titanium dioxide dye-sensitized solar cells (TiO2-DSSCs) based natural dyes using electrochemical impedance spectroscopy concept: A review. Solar Energy. 2020;207:1088–1121.

[19] Lee CP, Li CT, Ho KC. Use of organic materials in dye-sensitized solar cells. Materials Today. 2017;20:267–283.

[20] Lee DH, Lee MJ, Song HM, Song BJ, Seo KD, Pastore M, Anselmi C, Fantacci S, Angelis F, Nazeeruddin MK, Gretzel M, Kim HK. Organic dyes incorporating low-band-gap chromophores based on π-extended benzothiadiazole for dye-sensitized solar cells. Dyes and Pigments. 2011;91:192–198.

[21] Safaei-Ghomi J, Masoomi R, Hosseinpour M, Batooli H. Energy Production Using Dye-sensitized Solar Cells by TiO 2 Nanoparticles Fabricated with Several Natural Dyes. J Nanostruct. 2020;10:691–701.

[22] Tabacchi G, Fabbiani M, Mino L, Martra G, Fois E. The Case of Formic Acid on Anatase TiO2(101): Where is the Acid Proton. Angewandte Chemie - International Edition. 2019;58:12431–12434.

[23] Akila Y, Muthukumarasamy N, Agila S, Mallick TK, Senthilarasu S, Velauthapillai D. Enhanced performance of natural dye sensitised solar cells fabricated using rutile TiO2 nanorods. Optical Materials. 2016;58: 76–83.

[24] Sen A, Putra MH, Biswas AK, Behera AK, Groβ A. Insight on the choice of sensitizers/dyes for dye sensitized solar cells: A review. Dyes and Pigments. 2023;213:111087.

[25] Hayta S, Dogan G, Yuce E, Bagci E. Composition of the essential oil of two Salvia taxa (Salvia sclarea and Salvia verticillata subsp. verticillata) from Turkey. Natural Science and Discovery. 2015;1:56-

62.

[26] Nageen B, Sarfraz I, Rasul A, Hussain G, Rukhsar F, Irshad S, Riaz A, Selamoglu Z, Ali M. Eupatilin: a natural pharmacologically active flavone compound with its wide range applications. Journal of Asian Natural Products Research. 2020;22:1–16.

[27] Wang XF, Matsuda A, Koyama Y, Nagae H, Sasaki S, Tamiaki H, Wada Y. Effects of plant carotenoid spacers on the performance of a dye-sensitized solar cell using a chlorophyll derivative: Enhancement of photocurrent determined by one electron-oxidation potential of each carotenoid. Chemical Physics Letters. 2006;423:470–475.

[28] Inbarajan K, Sowmya S, Janarthanan B. Direct and soxhlet extraction of dyes from the peels of Allium cepa and its effective application in dye – Sensitized solar cells as sensitizer. Optical Materials. 2022;129:112487.

[29] Enhanced photovoltaic performance and stability Obi K, Frolova L, Fuierer P. Preparation and performance of prickly pear (Opuntia phaeacantha) and mulberry (Morus rubra) dye-sensitized solar cells. Solar Energy. 2020;208:312–320.

[30] Zhou H, Wu L, Gao Y, Ma T. Dye-sensitized solar cells using 20 natural dyes as sensitizers. Journal of Photochemistry and Photobiology A: Chemistry. 2011;219:188–194.

[31] Kristoffersen AS, Erga, SR, Velauthapillai D. Enhanced photostability of anthocyanin dye for increased efficiency in natural dye sensitized solar cells. Optik. 2021;227:166053.

[32] Hamadanian M, Safaei-Ghomi J, Hosseinpour M, Masoomi R, Jabbari V. Uses of new natural dye photosensitizers in fabrication of high potential dye-sensitized solar cells (DSSCs). Materials Science in Semiconductor Processing. 2014;27:733–739.

[33] Ramamoorthy R, Radha N, Maheswari G, Anandan S, Manoharan S, Williams, R. Betalain and anthocyanin dye-sensitized solar cells. Journal of Applied Electrochemistry. 2016;46:929–941.

[34] Calogero G, Barichello J, Citro I, Mariani P, Vesce L, Bartolotta A, Di-Carlo A, Di-Marco G. Photoelectrochemical and spectrophotometric studies on dye-sensitized solar cells (DSCs) and stable modules (DSCMs) based on natural apocarotenoids pigments. Dyes and Pigments. 2018;155:75–83.

[35] Ahmadi N, Yeganeh R, Valizadeh M, Valadbeigi T. Improvement of the fill factor characteristic of TiO2-based dye-sensitive solar cell using lichen Collema nigra. Optical Materials. 2022;638:112-131.

[36] Singh S, Maurya IC, Sharma S, Kushwaha SP, Srivastava P, Bahadur L. Application of new natural dyes extracted from Nasturtium flowers (Tropaeolum majus) as photosensitizer in dye-sensitized solar cells. Optik. 2021;243:167331.

[37] Aslan F, Esen H, Yakuphanoglu F. Al/P-Si/Coumarin:TiO2/Al Organic-Inorganic Hybrid Photodiodes: Investigation of Electrical and Structural Properties. Silicon. 2019;12:2149-2164.

[38] Luo P, Niu H, Zheng G, Bai X, Zhang M, Wang W. From salmon pink to blue natural sensitizers for solar cells: Canna indica L., Salvia splendens, cowberry and Solanum nigrum L. Spectrochimica Acta - Part A: Molecular and Biomolecular Spectroscopy. 2009;74:936–942.

[39] Richhariya G, Meikap BC, Kumar A. Review on fabrication methodologies and its impacts on performance of dye-sensitized solar cells. Environmental Science and Pollution Research. 2022;29:15233–15251.

[40] Aslan F. Increasing the photoelectric conversion efficiency of dye-sensitized solar cells by doping SrAl2O4:Eu+2,Dy+3 to TiO2-based photoanodes. Physica B: Condensed Matter. 2023;668:415267.

[41] Prakash P, Janarthanan B. Review on the progress of light harvesting natural pigments as DSSC sensitizers with high potency. Inorganic Chemistry Communications. 2023;152:110638.

[42] Sethy PP, Pani TK, Rout S. Structural and magnetic properties of Ni / C core – shell nanofibers prepared by one step co-axial electrospinning method. Journal of Materials Science: Materials in Electronics. 2023;807:1–15.

[43] Ge Z, Wan, C, Chen Z, Wang T, Chen T, Shi R, Yu S, Liu J. Investigation of the TiO2 nanoparticles aggregation with high light harvesting for high-efficiency dye-sensitized solar cells. Materials Research Bulletin. 2021;135: 111148.

[44] Du L, Furube A, Hara K, Katoh R, Tachiya M. Mechanism of particle size effect on electron injection efficiency in ruthenium dye-sensitized TiO2 nanoparticle films. Journal of Physical Chemistry C. 2010;114:8135–8143.

[45] Wali Q, Bakr ZH, Manshor NA, Fakharuddin A, Jose R. ScienceDirect SnO 2 – TiO 2 hybrid nanofibers for efficient dye-sensitized solar cells. 2016;132:395–404.

[46] Sayahi H, Aghapoor K, Mohsenzadeh F, Mohebi M, Darabi HR. TiO2 nanorods integrated with titania nanoparticles: Large specific surface area 1D nanostructures for improved efficiency of dye-sensitized solar cells (DSSCs). Solar Energy. 2021;215:311–320.

[47] Ayalew WA, Ayele DW. Dye-sensitized solar cells using natural dye as light-harvesting materials extracted from Acanthus sennii chiovenda flower and Euphorbia cotinifolia leaf. Journal of Science: Advanced Materials and Devices. 2016;1:488–494.

[48] Dayang S, Irwanto M, Gomesh N, Ismail B. Natural dyes from roselle flower as a sensitizer in dye-sensitized solar cell (DSSC). Indonesian Journal of Electrical Engineering and Computer Science. 2018;9:191–197.

[49] Güzel E, Arslan BS, Durmaz V, Cesur M, Tutar ÖF, Sarı T, Isleyen M, Nebioğlu M, Sisman I. Photovoltaic performance and photostability of anthocyanins, isoquinoline alkaloids and betalains as natural sensitizers for DSSCs. Solar Energy. 2018;173:34–41.

[50] Mozaffari SA, Saeidi M, Rahmanian R. Photoelectric characterization of fabricated dye-sensitized solar cell using dye extracted from red Siahkooti fruit as natural sensitizer. Spectrochimica

Acta - Part A: Molecular and Biomolecular Spectroscopy. 2015;142:226–231.

[51] Hajji S, Turki T, Boubakri A, Amor M, Mzoughi N. Study of cadmium adsorption onto calcite using full factorial experiment design. Desalination and Water Treatment. 2017;83:222–233.

[52] Subalakshmi K, Senthilselvan J, Kumar KA, Kumar SA, Pandurangan A. Solvothermal synthesis of hexagonal pyramidal and bifrustum shaped ZnO nanocrystals: natural betacyanin dye and organic Eosin Y dye sensitized DSSC efficiency, electron transport, recombination dynamics and solar photodegradation investigations. Journal of Materials Science: Materials in Electronics. 2017;20:10854.

[53] Bella F, Galliano S, Falco M, Viscardi G, Barolo C, Grätzel M, Gerbaldi C. Unveiling iodine-based electrolytes chemistry in aqueous dye-sensitized solar cells. Chemical Science. 2016;7:4880–4890.

[54] Chandra MI, Singh S, Srivastava P, Maiti B, Bahadur L. Natural dye extract from Cassia fistula and its application in dye-sensitized solar cell: Experimental and density functional theory studies. Optical Materials. 2019;90:273–280.

[55] Lohrasbi M, Pattanapanishsawat P, Isenberg M, Chuang, SS. Degradation study of dye-sensitized solar cells by electrochemical impedance and FTIR spectroscopy. IEEE Energytech. 2013;4:1–4.

[56] Rajan AK, Cindrella L. Studies on new natural dye sensitizers from Indigofera tinctoria in dye-sensitized solar cells. Optical Materials. 2019;88:39–47.

[57] Guo J, Cui X, Li S, Mao L, Liu Y, Huang W, Gong T, Wei X, Chen H, Yu B. One-step synthesis of mesoporous TiO2 film for high photon-to-electron transport efficiency in dye-sensitized solar cells. Journal of Alloys and Compounds. 2019;770:662–668.

[58] Kumar KA, Subalakshmi K, Senthilselvan J. Effect of mixed valence state of titanium on reduced recombination for natural dye-sensitized solar cell applications. Journal of Solid State Electrochemistry. 2016;20:1921–1932.

[59] Lim SP, Pandikumar A, Lim HN, Ramaraj R, Huang NM. Boosting photovoltaic performance of dye-sensitized solar cells using silver nanoparticle-decorated N,S-Co-doped-TiO2 photoanode. Scientific Reports. 2015;5:1–14.

[60] Aslan F. New natural dyes extracted by ultrasonic and soxhlet method: Effect on dye-sensitized solar cell photovoltaic performance. Optical and Quantum Electronics. 2024;56:1–22.

[61] Shalini S, Balasundara R, Prasanna S, Mallick TK, Senthilarasu S. Review on natural dye sensitized solar cells: Operation, materials and methods. Renewable and Sustainable Energy Reviews. 2015;51:1306–1325.

[62] Hamadanian M, Jabbari V, Gravand A, Asad M. Band gap engineering of TiO 2 nanostructure-based dye solar cells (DSCs) fabricated via electrophoresis. Surface and Coatings Technology. 2012;206:4531–4538.

[63] Narayan MR. Review: Dye sensitized solar cells based on natural photosensitizers. Renewable and Sustainable Energy Reviews. 2012;16:208–215.